Journal of Alloys and Compounds 480 (2009) 184–189

Contents lists available at ScienceDirect

Journal of Alloys and Compounds

journal homepage: www.elsevier.com/locate/jallcom

First-principles calculations and X-ray spectroscopy studies of the electronic structure of $CuWO_4$

O.Yu. Khyzhun*, V.L. Bekenev, Yu.M. Solonin

Frantsevych Institute for Problems of Materials Science, National Academy of Sciences of Ukraine, 3 Krzhyzhanivsky Street, UA-03142 Kyiv, Ukraine

ARTICLE INFO

Article history:
Received 21 January 2009
Received in revised form 29 January 2009
Accepted 29 January 2009
Available online 7 February 2009

Keywords:
Copper tungstate
$CuWO_4$
Electronic structure
Band-structure calculations
X-ray emission spectroscopy
X-ray absorption spectroscopy

ABSTRACT

First-principles self-consistent band-structure calculations of copper tungstate, $CuWO_4$, have been made using the full potential linearized augmented plane wave (FP-LAPW) method. Total and partial densities of states of the constituent atoms of $CuWO_4$ have been derived. The results obtained reveal that the valence band of $CuWO_4$ is dominated by contributions of the O 2p-like states, while the W 5d-like states are the main contributors into the conduction band of the tungstate. Additionally, the FP-LAPW calculations render that the W 5d- and Cu 3d-like states contribute mainly at the bottom and at the top of the valence band of $CuWO_4$, respectively. In the present work, the X-ray emission spectroscopy (XES) and X-ray absorption spectroscopy (XAS) methods were also employed to investigate experimentally the electronic structure of copper tungstate. For the mentioned compound, the XES bands reflecting the energy distribution of mainly the W 5d-, Cu 3d- and O 2p-like states were derived and compared on a common energy scale with the X-ray photoelectron valence-band spectrum. A rather good agreement of the experimental and theoretical data concerning electronic properties of $CuWO_4$ has been obtained in the present paper. Measurements of the energy shift of the XAS W L_{III} edge of $CuWO_4$ clearly demonstrate that tungsten atoms in copper tungstate are in the formal valence state +6.

1. Introduction

Copper tungstate, $CuWO_4$, is a well-known n-type semiconductor widely used as a laser host material, scintillation detectors, optical fibres, electrodes for photoelectrolysis, etc. [1–3]. $CuWO_4$ crystallizes in a triclinic (space group $P\bar{1}$) distorted wolframite-type structure [4], with unit-cell parameters $a = 4.7026$ Å, $b = 5.8389$ Å, $c = 4.8784$ Å, $\alpha = 91.677°$, $\beta = 92.469°$, $\gamma = 82.805°$ [5]. The findings by Gebert and Kihlborg [4,5] were confirmed lately by other investigators [6–8], as data listed in Table 1 reveal (it is necessary to mention that, Ruiz-Fuertes et al. [8] used a different setting to describe the structure of $CuWO_4$ as compared with those used in Refs. [5–7]). For single-crystal copper tungstate grown by the top-seeded solution growth method, no evidence of changes of the wolframite-type structure were found in high-pressure experiments up to 25 GPa, but large amounts of defects were apparent for the $CuWO_4$ crystal beyond 18 GPa [8]. Additionally, Forsyth et al. [7] have established that the distorted wolframite-type structure of copper tungstate is stable when lowering the temperature to 15 K.

The crystal structure of $CuWO_4$ is presented in Fig. 1. There are four non-equivalent positions for oxygen atoms (labelled as O(1), O(2), O(3), and O(4) [5]). The wolframite-type structure can be described as a framework of oxygen atoms in an approximately hexagonal close-packing with the cations occupying half of the octahedral sites. In the structure of $CuWO_4$, every metal atom is surrounded by six oxygen atoms: the ranges of the six M–O distances are within 1.961–2.450 Å for the CuO_6 octahedra and within 1.760–2.208 Å for the WO_6 octahedra [5]. Additionally, as established by Kihlborg and Gebert [5], copper and tungsten atoms form in $CuWO_4$ alternating sequence of layers laying between the oxygen sheets: infinite zigzag chains are formed by edge-sharing alternating WO_6 and CuO_6 octahedra. Doumerc et al. [9] have shown that the existence of two kinds of connections between the CuO_6 octahedra in the structure of $CuWO_4$ leads to alternating antiferromagnetic interactions along the chains. The magnetic unit cells ($2a$, b, c) are twice of the chemical unit (a, b, c) and identical to that of $FeWO_4$ [10]. This experimental finding was confirmed theoretically by Koo and Whangbo [11] based on calculations of spin–orbital interaction energies for spin dimmers of $CuWO_4$. Copper tungstate becomes antiferromagnetically ordered below 23.0(2) K [7].

As a representative member of tungstate and molybdate compounds crystallizing either in a scheelite or wolframite structure [12], $CuWO_4$ is considered to be an excellent material for the production of positive electrodes of rechargeable Li batteries [13] and for synthesis of almost porousless W–Cu pseudoalloys containing 10–35 mol.% of copper [14,15]. Hydrogen reduction of copper tungstate provides composite W–Cu powder products with a uniform, homogeneous dispersion of the metal phases [16]. Therefore,

---

* Corresponding author. Tel.: +380 44 424 33 64; fax: +380 44 424 21 31.
E-mail address: khyzhun@ipms.kiev.ua (O.Yu. Khyzhun).

0925-8388/$ – see front matter © 2009 Elsevier B.V. All rights reserved.
doi:10.1016/j.jallcom.2009.01.119

Table 1
Lattice parameters of copper tungstate, $CuWO_4$, as determined by different authors (triclinic structure, space group $P\bar{1}$).

a (Å)	b (Å)	c (Å)	α (°)	β (°)	γ (°)	V (Å^3)	Reference
4.7026(6)	5.8389(7)	4.8784(6)	91.677(9)	92.469(7)	82.805(10)	132.73	[5]
4.6964(9)	5.8287(10)	4.8736(7)	91.63(1)	92.44(1)	82.79(1)	132.2	[6]
4.694(1)	5.830(1)	4.877(1)	91.64(1)	92.41(2)	82.91(1)	132.29	[7][a]
4.709(7)	5.845(9)	4.884(7)	88.3(2)	92.5(2)	97.2(2)	133.2	[8]

[a] Measurements were made at 15 K.

different routes are applied for obtaining high-quality $CuWO_4$ in the form of bulk crystals (e.g., slow-cooled indirect flux reaction technique [17,18], recrystallization in an ampoule for chemical vapour transport [19]), films on different substrates (e.g., spray-sol–gel deposition [20], radio-frequency (RF) sputtering deposition [21]) or nanocrystalline powders possessing poor agglomeration of crystallites [22].

When measuring electrical conduction of a single-crystal copper tungstate, Bharati et al. [23] have shown that $CuWO_4$ is an intrinsic semiconductor with the band gap, E_g, 1.52 eV. A higher value of the band gap, mainly 2.06 eV, has been reported by Benko et al. [24] based on electrochemical measurements of $CuWO_4$. Further, Ruiz-Fuertes et al. [8] have established for $CuWO_4$ the indirect band-gap energy of 2.3 eV and its negative pressure coefficient (decreasing E_g with pressure up to 18 GPa following a quadratic function). The electronic structure of copper tungstate has been studied experimentally in Ref. [25]: for the compound under consideration, the X-ray photoelectron valence-band spectra with different energies of excitation were studied, the X-ray emission O 2p-like band and the near-edge X-ray absorption fine structure (NEXAFS) O 1s spectrum were derived, as well as the binding energies of the core-level electrons of the constituent atoms were measured. X-ray photoelectron measurements employing both Mg Kα excitation and photons with different energies (ranging from 100 to 500 eV) at the synchrotron facility of BESSY II (Berlin) have revealed a simple structure of the valence band of copper tungstate [25]. Both the X-ray photoelectron O 1s core-level binding energies measurements and the NEXAFS O 1s data reveal that negative charges of oxygen atoms are very similar in WO_3 and $CuWO_4$ [25]. The X-ray absorption chemical shift, ΔE, of the Cu K-edge in $CuWO_4$ with respect to its position in pure copper metal was measured by Pandey and Chetal [26].

First-principles calculations of some tungstate materials AWO_4 (A = Ca, Cd, Pb) [27–30] reveal some common features of electronic properties of these compounds. Partly, density-functional theory (DFT) calculations of Ca and Pb tungstates [27] and of $CdWO_4$ [28] using the linearized augmented plane wave (LAPW) method as well as studies of the electronic structure of $PbWO_4$ employing the generalized gradient approximation (GGA) within the CASTEP code [29,30] clearly demonstrate that in the compounds under consideration the O 2p-like states dominate the upper part of the valence band and have significant contributions throughout the main portion of the valence band, while the W 5d-like states are the main contributors near the bottom of the conduction band. However, some differences in the electronic structure of AWO_4 (A = Ca, Cd, Pb) compounds are obvious in the LAPW calculations [27,28]: the minimum band gap of $CaWO_4$ is located at the Γ point at the center of the Brillouin zone, while the minimum band gaps do not occur at Γ for Cd and Pb tungstates. As it has been established in Refs. [27,28], $CdWO_4$ possesses the minimum band gap at the Y point, which is located at the center of the Brillouin-zone boundary plane perpendicular to the b crystal axis, while $PbWO_4$ reveals band extrema at wave vectors away from the zone center (in the Σ and Δ directions) with possibly indirect band gaps. Recently different cluster approaches have been adopted to calculate the electronic structure of $PbWO_4$ [29–32], $CdWO_4$ [31] and $ZnWO_4$ [33] tungstates, mainly their optical and luminescence properties.

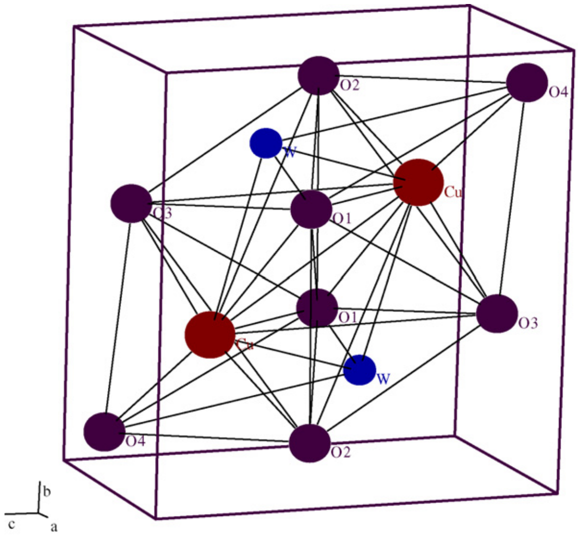

Fig. 1. Crystal structure of copper tungstate, $CuWO_4$: W, small balls; O, middle balls; Cu, large balls.

To the best of our knowledge, no theoretical band-structure calculations have been made so far for $CuWO_4$. Therefore, in the present paper we aim at a comprehensive study of the energy distribution of electronic states of different symmetries of the constituent atoms of copper tungstate. With this purpose, we have employed possibilities of the full potential linearized augmented plane wave (FP-LAPW) method as incorporated in the WIEN97 code [34] in order to study total density of states (DOS) and partial densities of states of the $CuWO_4$ compound. Additionally, the X-ray emission spectroscopy (XES) and X-ray absorption spectroscopy (XAS) methods have been used to study the energy distribution of some occupied valence and unoccupied states of the constituent atoms of copper tungstate.

2. Computational details

Calculations of electronic properties of $CuWO_4$ have been made using the first-principles self-consistent FP-LAPW method with the WIEN97 code [34]. In the present FP-LAPW calculations, lattice parameters and positions of the constituent atoms of $CuWO_4$ listed in Table 2 have been chosen in accordance with the crys-

Table 2
Positions of the constituent atoms of $CuWO_4$ used in the present FP-LAPW calculations.

Atom	Position of the atom		
	x	y	z
Cu	0.49533	0.65976	0.24481
W	0.02106	0.17348	0.25429
O(1)	0.2491	0.3535	0.4245
O(2)	0.2145	0.8812	0.4309
O(3)	0.7353	0.3803	0.0981
O(4)	0.7826	0.9097	0.0533

Table 3
Atomic orbitals used in the present FP-LAPW calculations of the electronic structure of $CuWO_4$.

Atom	Core electrons	Semi-core electrons	Valence electrons	Number of electrons involved in the present FP-LAPW calculations
Cu	$1s^2\ 2s^2\ 2p^6\ 3s^2$	$3p^6$	$3d^{10}\ 4s^1$	17
W	$1s^2\ 2s^2\ 2p^6\ 3s^2\ 3p^6\ 3d^{10}\ 4s^2\ 4p^6\ 4d^{10}$	$5s^2\ 5p^6\ 4f^{14}$	$5d^4\ 6s^2$	28
O	$1s^2$	$2s^2$	$2p^4$	6

tallography data determined for the compound by Kihlborg and Gebert [5]. The GGA approximation by Perdew et al. [35] was employed for calculations of the exchange-correlation potential. The muffin-tin (MT) sphere radii of the constituent atoms of $CuWO_4$ in the present calculations were assumed to be 0.873 Å for W and O and 1.005 Å for Cu. The $R_{\min}^{\mathrm{MT}}k_{\max}$ parameter, where $R_{\min}^{\mathrm{MT}}$ denotes the smallest MT sphere radius and $k_{\max}$ determines the value of the largest k vector in the plane wave expansion, equals to 10.0 (the charge density was Fourier expanded up to the value $G_{\max} = 14$). In the potential decomposition, the valence wavefunctions inside the MT spheres were expanded up to $l_{\max} = 3$. The basis function consists of the atomic orbitals of Cu, W, and O as listed in Table 3. A total number of semi-core and valence electrons (in addition to core electrons) per unit cell of $CuWO_4$ equals to 138 in the present calculations. Integration through the Brillouin zone was carried out using the tetrahedron method by Blöchl et al. [36]. The Brillouin-zone sampling has been done using 92 k-points within the irreducible part of the zone. The iteration process was checked taking into account changes of total energy and the calculations were interrupted when for three following iterations the change of total energy was less than 1×10^{-4} Ry ($\sim 1 \times 10^{-5}$ eV).

3. Experimental

Details of specimen preparation were reported in Refs. [25,37]. Briefly, copper tungstate, $CuWO_4$, studied in the present paper was obtained by solid-state reaction of CuO and the usual monoclinic form of WO_3, according to the relation $CuO + WO_3 = CuWO_4$. The solid-state reaction was carried out on air at 800 °C. A conventional X-ray diffraction analysis carried out with a DRON-3 diffractometer using Cu Kα radiation has rendered [37,38] that unit-cell parameters of the powder $CuWO_4$ tungstate under study are in good agreement with the results of Kihlborg and Gebert [5].

The ultrasoft X-ray emission Cu Lα ($L_{III} \rightarrow M_{IV,V}$ transition) band reflecting mainly the energy distribution of the Cu d-like states, in $CuWO_4$ under consideration was recorded in the second order of reflection using an RSM-500 spectrometer equipped with a diffraction grating possessing 600 lines/mm and a radius of curvature of $R \approx 6$ m. The detector was a secondary electron multiplier VEU-6 with a CsI photocathode. The base pressure in the spectrometer analyzing chamber was less than 1×10^{-6} Pa. Operating conditions of an electron gun in the present experiments were the following: accelerating voltage, $U_a = 6$ kV; anode current, $I_a = 10$ mA. The spectrometer energy resolution was about 0.3 in the energy region corresponding to the position of the Cu Lα band. The technique of band acquisition and preparation of the powder $CuWO_4$ tungstate for the experiment was similar to that used in Ref. [39].

The fluorescent X-ray W Lβ$_5$ emission band ($L_{III} \rightarrow O_{IV,V}$ transition) reflecting primarily the W 5d-like states was obtained using a DRS-2M spectrograph (the resolution was estimated to be better than 0.4 eV) in the second order of reflection from the (0 0 0 1) plane of a quartz crystal prepared according to Johann (see Ref. [40] for details). The method of the W Lβ$_5$ band acquisition was analogous to that used in Ref. [41]. An X-ray BHV-7 tube with a gold anode operating at $U_a = 45$ kV and $I_a = 75$ mA was used as a source of spectrum excitation. At the above experimental conditions, the intensity of the X-ray W Lβ$_5$ emission band was found to be rather low in $CuWO_4$: the band presented in the present paper was obtained with accumulative time of about 240 h.

The XAS W L_{III} edge reflecting the energy distribution of the unoccupied W d-like states was obtained in $CuWO_4$ with a KRUS-1 spectrometer using scintillation recording of the X-ray radiation intensity and employing the method of 'a variable field of absorption' (see, e.g., Ref. [41]). The technique was analogous to that used earlier when studying the edges in tungsten oxides [42,43]. As a disperse element, a quartz crystal with the $(13\bar{4}0)$ reflecting plane and a radius of curvature of $R = 872$ mm was used. The absorber covering half of the rotating sample cell was made in the form of a thin film of $CuWO_4$ under study with a wax binder. As a source of primary excitation of the XAS W L_{III} edge, a BSV-23 X-ray tube operating at $U_a = 14$ kV and $I_a = 40$ mA was used.

4. Results and discussion

Fig. 2 compares total DOS of $CuWO_4$ with total densities of states of the constituent atoms of the compound. Zero of energy has been taken at the top of the last occupied band as it was suggested for tungstate materials AWO_4 (A = Ca, Cd, Pb) in LAPW calculations [27,28]. In Fig. 2 we present total DOS of $CuWO_4$ ranging between −20.7 eV below the top of the valence band to 12.2 eV towards the upper sub-bands of the conduction band. As one can see from Fig. 2, the lowest band obtained in the present FP-LAPW calculations of $CuWO_4$ ranges from −17.2 to −19.6 eV and originates mainly from contributions of the O 2s-like states with minor contributions of the W 5p-like states (Fig. 3). The mention band, as Fig. 2 displays, can be divided on three sub-bands, mainly *a*, *b*, and *c*. Among these bands, the lowest one centered at −19.2 eV is composed mainly of the O 2s-like states of the O(2) atoms, with smaller contributions of the analogous states of the other oxygen atoms (Fig. 4). Figs. 2 and 4 reveal that the O 2s-like states of the O(1), O(2) and O(3) atoms contribute in almost equal proportions into the sub-band *b* centered at −18.15 eV. Minor contributions of the W 5p- and W 5d-like states into this sub-band are also detected by the present FP-LAPW calculations (Fig. 3). Finally, the main contributors into the sub-band

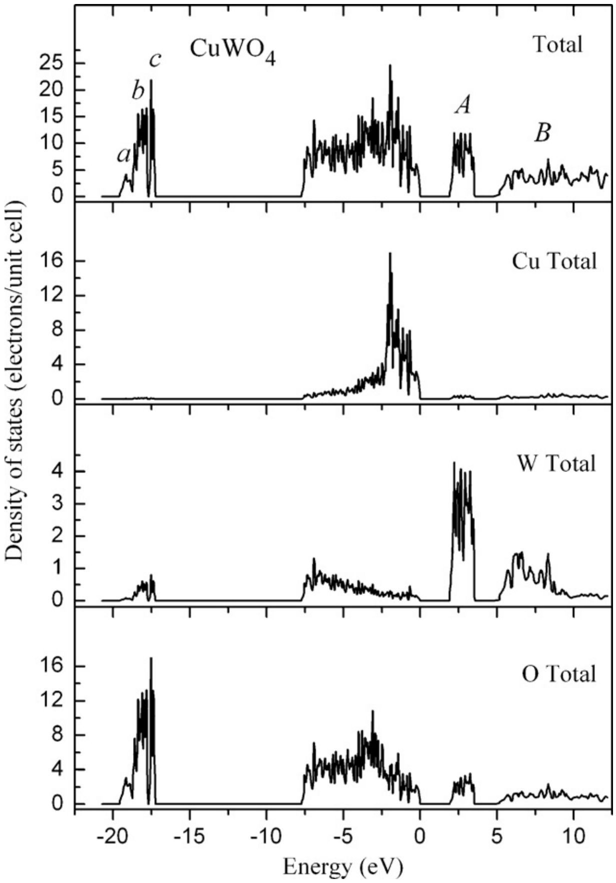

Fig. 2. Total DOS of $CuWO_4$ and total densities of states of the constituent atoms of the compound.

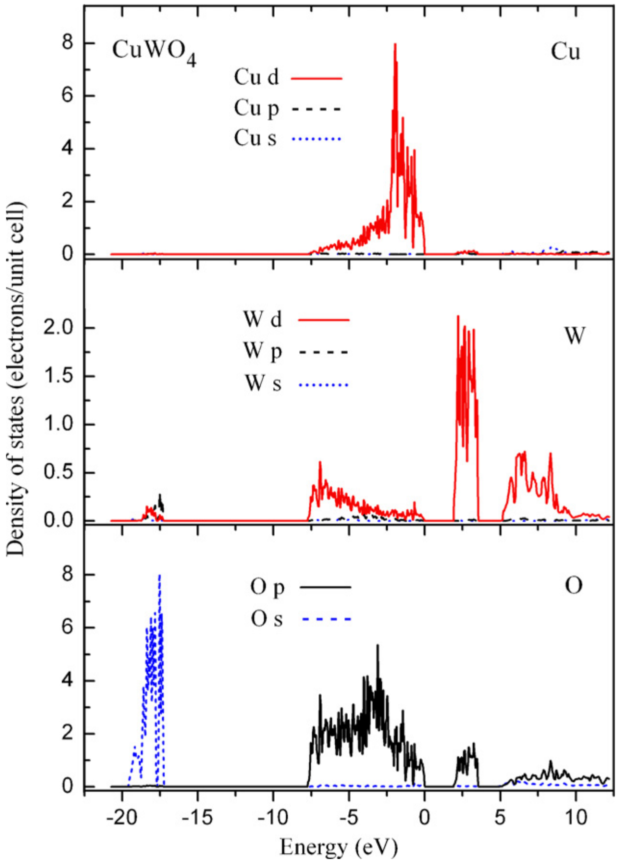

Fig. 3. Partial densities of states of the constituent atoms of CuWO$_4$.

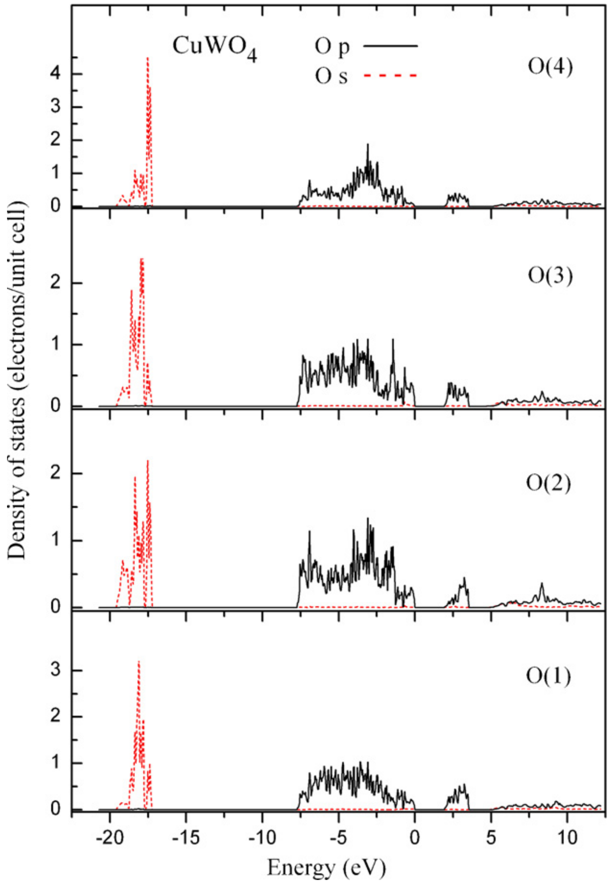

Fig. 4. Partial densities of states of oxygen atoms of CuWO$_4$.

c centered at −17.45 eV are the O 2s-like states of the O(2) and O(4) atoms, with smaller contributions of the O 2s-like states of the O(1) and O(3) atoms as well as of the W 5p-like states (cf. Figs. 2–4).

From Figs. 2 and 3 it is obvious that the valence band of CuWO$_4$ ranges from 0 to −7.7 eV and it is composed mainly of the Cu 3d-, W 5d- and O 2p-like states. As can be seen from Fig. 3, the W 5d- and Cu 3d-like states contribute mainly into the bottom and the upper part of the valence band, respectively, while the O 2p-like states contribute significantly throughout the valence-band region of CuWO$_4$. From Fig. 4 it is apparent that contributions of the O 2p-like states into the valence band of copper tungstate depend on the position of oxygen atoms in the unit cell of the compound as follows: the O(1) and O(3) atoms contribute mainly into the central and lower parts of the valence band, the O(2) atoms contribute significantly into the whole valence-band region except of its upper part, and the O(4) atoms contribute mainly into the central part of the valence band. From calculations of the areas under curves presented in Fig. 3 we can conclude that the main contributors into the valence band of CuWO$_4$ are the O 2p-like states.

Fig. 2 reveals that a rather narrow sub-band *A* ranging from 1.9 to 3.6 eV and separated from a rather broad upper sub-band *B* by a gap of 1.5 eV width can be distinguished at the bottom of the conduction band of CuWO$_4$. From Fig. 3 it is apparent that the bottom of the conduction band (the sub-band *A*; see Fig. 2) is composed mainly of the W 5d-like states with slightly smaller contributions of the O 2p-like states. Fig. 3 renders that the W 5d- and O 2p-like states are hybridized within the sub-band *A* of the conduction band of copper tungstate under study. Further, the W 5d- and O 2p-like states are also principal contributors to the higher sub-band *B* of the unoccupied states of CuWO$_4$. From Figs. 2 and 3 one can conclude that contributions of states associated with copper into the conduction band of CuWO$_4$ are rather small. It should be mentioned that contributions of the W 6s- and W 5p-like states (see Fig. 3) as well as of the W 4f-like states (not presented in Fig. 3) are very minor throughout the valence-band and conduction-band regions.

The above results seem to be in good agreement with those obtained in DFT calculations of electronic properties of tungstates AWO$_4$ (A = Ca, Cd, Pb) using the LAPW method [27,28]. For instance, the valence-band width was found to be about 7 eV for CdWO$_4$ with the wolframite-type structure [28]. This value is very close to that (7.7 eV) obtained in the present calculations of CuWO$_4$. For scheelite-type materials CaWO$_4$ and PbWO$_4$ the LAPW calculations by Zhang et al. [27] reveal somewhat smaller magnitudes of the valence-band widths, mainly 5 and 5.5 eV for Ca and Pb tungstate, respectively. Further, the LAPW data [27,28] clearly demonstrate that the W 5d-like states contribute mainly near the bottom of the valence band of the AWO$_4$ (A = Ca, Cd, Pb) compounds, while the dominant contributions of these states occur in the lower portion of the conduction band where they are split by the approximately octahedral crystal field on two main groups of states. These peculiarities are characteristic also of CuWO$_4$ as one finds from the density-of-states features of the compound presented in Figs. 2 and 3. Additionally, the O 2p-like states are the main contributors to the valence band of tungstates AWO$_4$ (A = Ca, Cd, Pb) [27,28]; this conclusion is also true for CuWO$_4$ as it was discussed above. It is worth to mention that, XPS studies and relativistic molecular orbital calculations of the electronic structure made by Itoh et al. [44] for scheelite-like Pb, Ca and Ba tungstates as well as for wolframite-like CdWO$_4$ and ZnWO$_4$ compounds also demonstrate that the valence and conduction bands of these oxides are mainly composed of the O 2p and W 5d states, respectively. Finally, like in the present FP-LAPW calculations of $CuWO_4$ (cf. Figs. 2–4), Abraham et al. [28] have also revealed a three-peak structure of the O 2s-like sub-band of the wolframite-type $CdWO_4$ compound. Since the similar calculations of electronic properties of scheelite-type $CaWO_4$ and $PbWO_4$ tungstates clearly demonstrate a single-peak O 2s-like sub-band [27], we can conclude that the three-peak structure of the O 2s-like sub-band originates due to the lower local symmetry and wider distribution of ligand bond lengths in the wolframite-type $CuWO_4$ compound as compared with those of scheelite-like Ca and Pb tungstates.

As it has been already mentioned above, the present FP-LAPW calculations show (Fig. 3) that the top of the valence band of $CuWO_4$ is dominated by contributions of copper states (mainly the Cu 3d-like states), however Cu states do not contribute significantly into the conduction band of the compound. Zhang et al. [27] have shown that Pb atoms contribute insignificantly into the total DOS curve within the energy region corresponding to the positions of the valence and conduction bands of $PbWO_4$, while Ca atoms contribute dominantly into the upper portion of the conduction band of $CaWO_4$ (above 7 eV with respect to the top of the valence band). Contributions of Cd atoms dominate the bottom of the valence band of $CdWO_4$ tungstate, however no significant Cd contributions throughout the conduction band of the compound were detected by LAPW calculations [28]. The above results reveal that the influence of the A atom on electronic properties of the mentioned AWO_4 tungstates depends significantly on its position in the Periodic Table. This statement confirms the similar conclusion recently suggested by Lacomba-Perales et al. [45] based on optical-absorption and reflectance measurements at room temperature in a number of single-crystal AWO_4 tungstates (A = Ba, Ca, Cd, Cu, Pb, Sr, and Zn).

It should be mentioned that, the present FP-LAPW calculations gives the value 1.9 eV for the energy gap, E_g, of $CuWO_4$. It is well known that first-principles calculations made within the GGA approximation [35] underestimate somewhat the energy gap of semiconductors and insulators [46–49]. Therefore, we can consider that the value $E_g = 1.9$ eV obtained theoretically in the present FP-LAPW calculations for $CuWO_4$ is in good agreement with experimentally measured values $E_g = 2.3$ eV [8] and $E_g = 2.06$ eV [24].

The experimental X-ray emission W Lβ_5 and Cu Lα bands recorded for $CuWO_4$ tungstate are shown in Fig. 5. In this figure, for comparison, the X-ray emission O Kα band (reflecting the energy distribution of the O 2p-like states) and the XPS valence-band spectrum that were derived for copper tungstate under consideration in Ref. [25] are also presented. All the mentioned X-ray emission spectra of $CuWO_4$ are matched in Fig. 5 with the XPS valence-band spectrum provided that a common energy scale is used. It should be mentioned that, comparison on a common energy scale of the X-ray emission W Lβ_5, Cu Lα and O Kα bands and the XPS valence-band spectrum of $CuWO_4$ was made taking into account binding energies of the W $4f_{7/2,5/2}$, Cu $2p_{3/2,1/2}$ and O 1s core-level electrons derived for this compound in our previous paper [25] and using measurements of photon energies of suitable inner X-ray lines. The method of matching the X-ray emission bands on a common energy scale is analogous to that applied successfully when studying the electronic structure of a number of transition metal oxides [43,50–52].

Results of studies of the X-ray emission bands presented in Fig. 5 indicate that the main contributions of the W 5d- and O 2p-like states are observed at the bottom and near the top of the valence band of $CuWO_4$, respectively, with contributions of the mentioned states throughout other portions of the valence band of the compound. However, the energy position of the Cu Lα band in Fig. 5 reveals that the top of the valence band of $CuWO_4$ is dominated by contributions of the Cu 3d-like states. The above experimental results confirm the data of the FP-LAPW calculations of copper tungstate presented in Figs. 2 and 3.

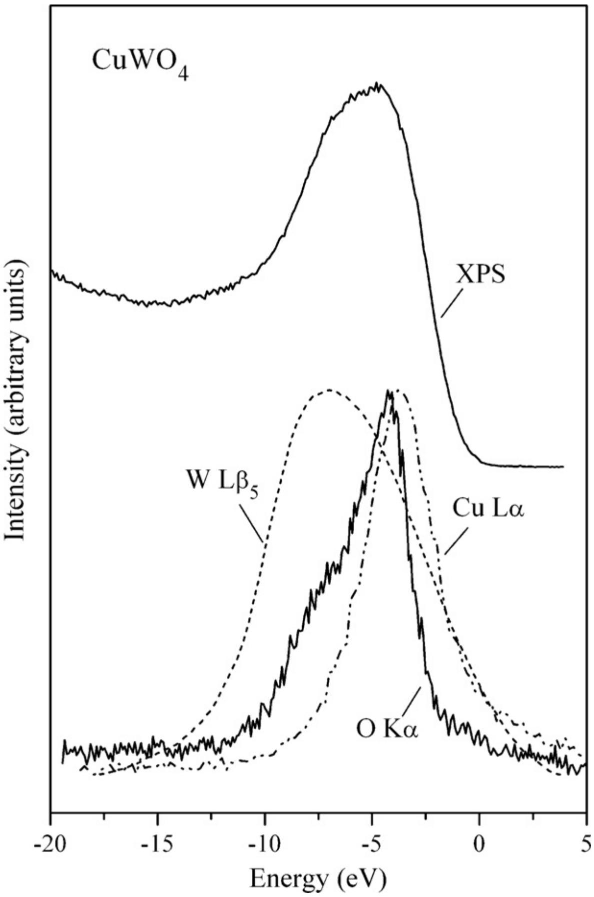

Fig. 5. The X-ray emission W Lβ_5, Cu Lα and O Kα bands of $CuWO_4$ matched on a common energy scale with the XPS valence-band spectrum of the compound (*Note*: The XPS valence-band spectrum was excited by photons with energy of 400 eV as reported in Ref. [25]).

Fig. 6 depicts the XAS W L_{III} edge of $CuWO_4$. For comparison, in this figure the analogous edges of pure metallic tungsten and the monoclinic form of WO_3 are also shown. From Fig. 6 it is apparent that the inflection point of the W L_{III} edge of copper tungstate reveals a high-energy shift compared with its position in metallic tungsten. The magnitudes of high-energy shifts of the inflection points of the W L_{III} edges of $CuWO_4$ and WO_3 are one and the same within the present experimental errors. When studying the X-ray absorption W L_{III} edges of substoichiometric tungsten oxides [42] it has been established that the almost monotonous high-energy shift of the inflection point of the edges occurs with increasing content of oxygen atoms in the sequence $WO_2 \rightarrow WO_3$. This shift could be explained by increasing the positive effective charge on tungsten atoms in the above sequence of oxides [42]. Therefore, the coincidence of magnitudes of the high-energy shifts of the inflection points of the XAS W L_{III} edges of $CuWO_4$ and WO_3 indicates that tungsten atoms in $CuWO_4$ are in the formal valence state +6. This finding is in agreement with data, which have appeared in the literature regarding AWO_4 tungstates [12,27,53–55]. It is well known that the structure of the AWO_4 compounds can be represented as highly ionic with A^{2+} cations and tetrahedral ${WO_4}^{2-}$ anions. Additionally, the ${WO_4}^{2-}$ anions are themselves can be viewed as highly ionic with $W^{\beta+}$ and $O^{\gamma-}$, where $4\gamma - \beta = 2$ [27]. Therefore, in the case of the absence of covalent bonding in the AWO_4 compounds, β and γ would take the values 6 and 2, respectively [27]. This conclusion is in agreement with the present XAS W L_{III} measurements for $CuWO_4$ as discussed above.

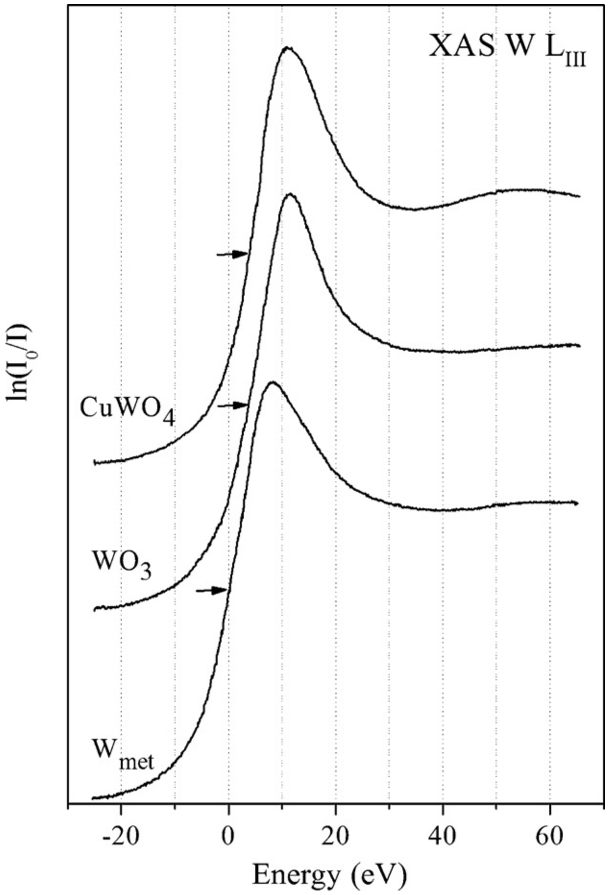

Fig. 6. The W L_{III} absorption spectrum of $CuWO_4$; for comparison, the spectra of pure metallic tungsten and the monoclinic form of WO_3 are also presented (*Note*: The arrows depict the energy positions of the inflection points of the XAS edges).

5. Conclusions

The present first-principles FP-LAPW calculations of $CuWO_4$ reveal that the O 2p-like states are the main contributors into the valence band of the compound, while the conduction band is dominated by contributions of the W 5d-like states. Additionally, the W 5d- and Cu 3d-like states contribute mainly at the bottom and at the top of the valence band of copper tungstate, respectively, while significant portions of contributions of the O 2p-like states throughout the valence-band region is characteristic of the electronic structure of $CuWO_4$. Comparison on a common energy scale of the X-ray emission bands reflecting the energy distribution of mainly the W 5d-, Cu 3d- and O 2p-like states of $CuWO_4$ confirm experimentally the above FP-LAPW theoretical findings. Common features of electronic properties of copper tungstate derived in the present paper are in agreement with data of similar LAPW calculations of Zhang et al. [27] and Abraham et al. [28] carried out for tungstates AWO_4 (A = Ca, Cd, Pb). Evaluation of the energy shift of the inflection point of the XAS W L_{III} edge of $CuWO_4$ renders that tungsten atoms are in the formal valence state +6 in copper tungstate under consideration.

References

[1] M.A. Butler, J. Appl. Phys. 48 (1977) 1914–1920.
[2] S.A.T. Redfern, Phys. Rev. B 48 (1993) 5761–5765.
[3] P.K. Pandey, N.S. Bhave, R.B. Kharat, Mater. Lett. 59 (2005) 3149–3155, and references therein.
[4] E. Gebert, L. Kihlborg, Acta Chem. Scand. 21 (1967) 2575–2576.
[5] L. Kihlborg, E. Gebert, Acta Crystallogr. B 26 (1970) 1020–1025.
[6] S. Klein, H. Weitzel, J. Appl. Crystallogr. 8 (1975) 54–59.
[7] J.B. Forsyth, C. Wilkinson, A.I. Zvyagin, J. Phys.: Condens. Matter 3 (1991) 8433–8440.
[8] J. Ruiz-Fuertes, D. Errandonea, A. Segura, F.J. Manjón, Zh. Zhu, C.Y. Tu, High Pressure Res. 28 (4) (2008) 565–570.
[9] J.P. Doumerc, J.M. Dance, J.P. Chaminade, M. Pouchard, P. Hagenmuller, M. Krussanova, Mater. Res. Bull. 16 (8) (1981) 985–990.
[10] H. Weitzel, Solid State Commun. 8 (24) (1970) 2071–2072.
[11] H.-J. Koo, M.-H. Whangbo, Inorg. Chem. 40 (9) (2001) 2161–2169.
[12] S.V. Borisov, N.V. Podberezskaya, Stable Cationic Motives in Structures of Fluorides and Oxides, Nauka, Novosibirsk, 1984 (in Russian).
[13] F. Bonino, B. Di Pietro, B. Rivolta, B. Scrosati, J. Power Sources 2 (1977) 265–272.
[14] V.V. Skorokhod, Yu.M. Solonin, N.I. Filippov, Sov. Powder Metall. Metal Ceram. 22 (9) (1983) 696–699.
[15] Yu.M. Solonin, Yu.G. Grivalov, N.I. Filippov, Sov. Powder Metall. Metal Ceram. 23 (10) (1984) 751–755.
[16] L.P. Dorfman, D.L. Houck, M.J. Scheithauer, J.N. Dann, H.O. Fassett, J. Mater. Res. 16 (4) (2001) 1096–1102.
[17] S.K. Arora, T. Mathew, N.M. Batra, J. Cryst. Growth 88 (3) (1988) 379–382.
[18] S.K. Arora, T. Mathew, N.M. Batra, J. Phys. Chem. Solids 50 (7) (1989) 665–668.
[19] F. Yu, U. Schanz, E. Schmidbauer, J. Cryst. Growth 132 (3–4) (1993) 606–608.
[20] M.A. Damián, Y. Rodriguez, J.L. Solis, W. Estrada, Thin Solid Films 444 (1–2) (2003) 104–110.
[21] C.-L. Li, Z.-W. Fu, Electrochim. Acta 53 (12) (2008) 4293–4301.
[22] A. Sen, P. Pramanik, J. Eur. Ceram. Soc. 21 (6) (2001) 745–750.
[23] R. Bharati, R.A. Singh, Y.P. Yadava, J. Mater. Sci. Lett. 2 (1983) 623–624.
[24] F.A. Benko, C.L. MacLaurin, F.P. Koffyberg, Mater. Res. Bull. 17 (1982) 133–136.
[25] O.Yu. Khyzhun, T. Strunskus, S. Cramm, Yu.M. Solonin, J. Alloys Compd. 389 (2005) 14–20.
[26] S.K. Pandey, A.R. Chetal, Phys. B: Condens. Matter 179 (1) (1992) 55–58.
[27] Y. Zhang, N.A.W. Holzwarth, R.T. Williams, Phys. Rev. B 57 (1998) 12738–12750.
[28] Y. Abraham, N.A.W. Holzwarth, R.T. Williams, Phys. Rev. B 62 (2000) 1733–1741.
[29] L. Tingyu, S. Jianqi, Z. Qiren, Z. Songlin, Nucl. Instrum. Methods Phys. Res. A 560 (2006) 460–463.
[30] Z. Xiuyan, Z. Qiren, L. Tingyu, Solid State Commun. 142 (2007) 647–650.
[31] Yu.A. Hizhnyi, S.G. Nedilko, T.N. Nikolaenko, Nucl. Instrum. Methods Phys. Res. A 537 (2005) 36–39.
[32] Z. Yi, T. Liu, Q. Zhang, Y. Sun, J. Electron. Spectrosc. Relat. Phenom. 151 (2006) 140–143.
[33] T.N. Nikolaenko, Yu.A. Hizhnyi, S.G. Nedilko, J. Lumin. 128 (2008) 807–810.
[34] P. Blaha, K. Schwarz, J. Luitz, WIEN97, A Full Potential Linearized Augmented Plane Wave Package for Calculating Crystal Properties, Technical University, Vienna, 1999 (Improved and update Unix version of the original copyrighted WIEN-code, which was published by P. Blaha, K. Schwarz, P. Sorantin, S.B. Trickey, Comput. Phys. Commun. 59 (1990) 399–415).
[35] J.P. Perdew, S. Burke, M. Ernzerhof, Phys. Rev. Lett. 77 (1996) 3865–3868.
[36] P.E. Blöchl, O. Jepsen, O.K. Andersen, Phys. Rev. B 49 (1994) 16223–16233.
[37] O.Yu. Khyzhun, Yu.M. Solonin, Powder Metall. Metal Ceram. 39 (2000) 287–294.
[38] O.Yu. Khyzhun, D.Sc. Thesis, Frantsevych Institute for Problems of Materials Science, National Academy of Sciences of Ukraine, Kyiv, 2005.
[39] O.Yu. Khyzhun, Metallofiz. Noveishie Tekhnol. 27 (6) (2005) 805–816.
[40] A. Meisel, G. Leonhardt, R. Szargan, X-Ray Spectra and Chemical Binding, Springer-Verlag, Berlin/Heidelberg, 1989.
[41] O.Yu. Khyzhun, Ya.V. Zaulychny, E.A. Zhurakovsky, J. Alloys Compd. 244 (1996) 107–112.
[42] O.Yu. Khyzhun, J. Alloys Compd. 305 (2000) 1–6.
[43] O.Y. Khyzhun, Y.M. Solonin, J. Phys.: Conf. Ser. 61 (2007) 534–539.
[44] M. Itoh, N. Fujita, Y. Inabe, J. Phys. Soc. Jpn. 75 (2006), 084705-1–084705-8.
[45] R. Lacomba-Perales, J. Ruiz-Fuertes, D. Errandonea, D. Martínez-García, A. Segura, Eur. Phys. Lett. 83 (2008) 37002.
[46] M. Städele, J.A. Majewski, P. Vogl, A. Görling, Phys. Rev. Lett. 79 (1997) 2089–2092.
[47] J. Kohanoff, N.I. Gidopoulos, in: S. Wilson (Ed.), Handbook of Molecular Physics and Quantum Chemistry, vol. 2, John Wiley & Sons Ltd., Chichester, 2003, pp. 532–568 (Part 5, Chapter 26).
[48] M. Grüning, A. Marini, A. Rubio, Phys. Rev. B 74 (2006) 161103-1–161103-4.
[49] A.J. Cohen, P. Mori-Sánchez, W. Yang, Phys. Rev. B 77 (2008) 115123-1–115123-6.
[50] O.Yu. Khyzhun, T. Strunskus, W. Grünert, Ch. Wöll, J. Electron. Spectrosc. Relat. Phenom. 149 (2005) 45–50.
[51] O.Yu. Khyzhun, V.L. Bekenev, Yu.M. Solonin, J. Alloys Compd. 459 (2008) 22–28.
[52] O.Yu. Khyzhun, V.L. Bekenev, V.V. Atuchin, A.K. Sinelnichenko, L.I. Isaenko, J. Alloys Compd. (2008), doi:10.1016/j.jallcom.2008.10.144.
[53] L.G. Sillén, A.-L. Nylander, Arkiv för Kemi, Mineralogi och Geologi (Stockholm) 17A (4) (1943) 25–27.
[54] A.F. Wells, Structural Inorganic Chemistry, 5th ed., Oxford Science Publications, Oxford, 1984 (ISBN 0-19-855370-6).
[55] E. Wiberg, A.F. Holleman, Inorganic Chemistry, Elsevier, 2001 (ISBN 0123526515).